

## Article

# Polymetallic Group 4 Complexes: Catalysts for the Ring Opening Polymerisation of *rac*-Lactide

David T. Jenkins, Eszter Fazekas, Samuel B. H. Patterson, Georgina M. Rosair , Filipe Vilela   
and Ruairaidh D. McIntosh \* 

Institute of Chemical Sciences, Heriot-Watt University, Edinburgh EH14 4AS, UK; dj32@hw.ac.uk (D.T.J.); e.fazekas@hw.ac.uk (E.F.); sp10@hw.ac.uk (S.B.H.P.); g.m.rosair@hw.ac.uk (G.M.R.); f.vilela@hw.ac.uk (F.V.)

\* Correspondence: r.mcintosh@hw.ac.uk

**Abstract:** Five novel air- and moisture-stable polymetallic Ti and Zr amino acid-derived amine bis(phenolate) (ABP) complexes were synthesised and fully characterised, including X-ray crystallographic studies. The reaction of the ABP proligands with Ti or Zr alkoxides has resulted in the formation of polymetallic aggregates of different nuclearity. The steric bulk on the pendant arm of the ligand was found to play a critical role in establishing the nuclearity of the aggregated complex. Sterically, less-demanding groups, such as H or Me, facilitated the formation of tetrametallic Ti clusters, bridged by carboxylate groups, while increased steric bulk (<sup>t</sup>Bu) led to the formation of binuclear  $\mu$ -oxo-bridged species. The isolated complexes were employed as catalysts for the ring opening polymerisation (ROP) of *rac*-lactide. Overall, the Ti catalysts were all active with the smaller, bimetallic Ti aggregates exhibiting relatively faster rates. A monometallic, bis(ABP) Zr complex was found to exert remarkable ROP activity, albeit with limited control over the tacticity and molecular weight distribution of the polymer. A further oxo-bridged Zr cluster was shown to display a previously unprecedented trimetallic structure and achieved a moderate rate in the ROP of *rac*-lactide.



**Citation:** Jenkins, D.T.; Fazekas, E.; Patterson, S.B.H.; Rosair, G.M.; Vilela, F.; McIntosh, R.D. Polymetallic Group 4 Complexes: Catalysts for the Ring Opening Polymerisation of *rac*-Lactide. *Catalysts* **2021**, *11*, 551. <https://doi.org/10.3390/catal11050551>

Academic Editor: Gregory A. Solan

Received: 1 April 2021  
Accepted: 26 April 2021  
Published: 27 April 2021

**Publisher's Note:** MDPI stays neutral with regard to jurisdictional claims in published maps and institutional affiliations.



**Copyright:** © 2021 by the authors. Licensee MDPI, Basel, Switzerland. This article is an open access article distributed under the terms and conditions of the Creative Commons Attribution (CC BY) license (<https://creativecommons.org/licenses/by/4.0/>).

**Keywords:** ROP; lactide; zirconium; titanium; amine bis(phenolate) ABP; catalysis; homogenous; polymetallic

## 1. Introduction

The ring-opening polymerisation (ROP) of cyclic esters has been intensely studied in recent years as attention has moved towards creating biodegradable plastics that can be produced from renewable sources [1,2]. The most commonly studied sustainable polymer is poly(lactic acid) (PLA), which is typically produced through the ROP of lactide (LA). PLA has a number of useful properties that have allowed it to be used extensively in food packaging films and medical implants [3]. The catalytic ROP of lactide, commonly carried out using homogenous Lewis acidic metal complexes, can be selectively controlled via two possible mechanisms; chain-end control and site control. Chain-end control occurs when the coordination of the incoming monomer is influenced by the chirality of the terminal monomer unit, if the structure of the catalyst/initiator controls the reaction, it is termed site control [4,5]. Structurally induced chirality, from the unique coordination mode of ligand to the metal centre, results in complexes that exhibit chain-end control, with some examples working through a proposed dynamic enantiomeric site control mechanism [6–8]. Alternatively, the use of a ligand that contains a chiral centre can initiate a passive enantiomeric site control mechanism, thus the arrangement of the chiral centres can be tailored and controlled through ligand design [6,9–11]. Salen and amine tris/bis(phenolate) ligands have been widely studied for this purpose and have shown great capacity for influencing the tacticity of the polymer through ligand design [12–16]. Lewis acidic metals, such as Al [17], Ti [18], Zn [19], Ge [8], Y [20], Zr [21], Sn [22], and Hf [23], are the most commonly used catalysts for the ROP of lactide. Of the group 4 metals, Zr is reported to achieve the highest turnover frequencies (TOF) and greatest control over tacticity and dispersity

(*D*) [7,24]. However, many Zr catalysts (similar to many other highly active ROP catalysts) are relatively unstable in the presence of air and moisture; therefore, they are not yet suitable for industrial applications. To provide extra stability to metal complexes, we investigated the incorporation of amino acids into amine bis(phenolate) (ABP) proligands [25,26]. The pendant carboxylic acid moieties formed bridging carboxylate groups upon reaction with Ti precursors affording stable polynuclear structures (Figure 1). The nature of the pendant arm has been shown to influence both molecular structure and catalyst activity, therefore, we anticipate this could play a dual role in the ROP reactions [27]. Unsubstituted (glycine) pendant arms allowed the formation of tetranuclear clusters; however, it was found that variation in the pendant arm influenced the formation of alternative aggregates. These varied in size and were shown to dynamically convert in solution (Figure 1). The carboxylate bridges provided additional stability, which we attribute to providing their air- and moisture-tolerance, while maintaining the high reactivity in the ROP of *rac*-lactide [25,26].

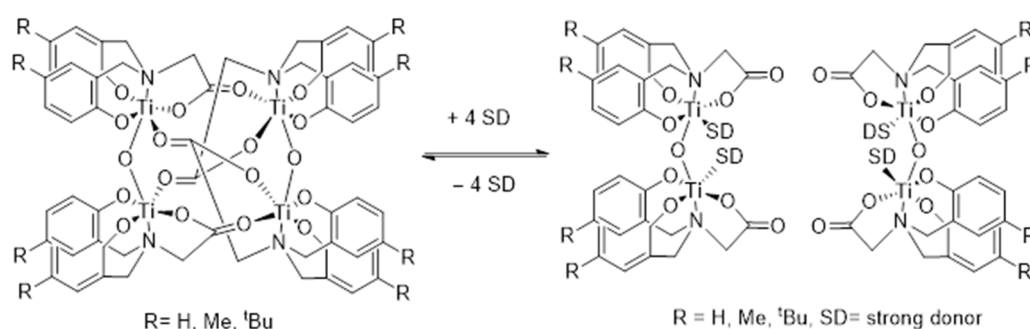


**Figure 1.** Dissociation between tetranuclear Ti cluster ( $(\text{Ti}_2\text{O})_2\text{L}_4$ ) (left) and binuclear variant (right).

Expanding the library of our previously reported polymetallic Ti clusters, this work explores the synthesis of novel Ti and Zr complexes using a broader range of amino acid-derived ABP proligands. The delicate influence of the different carboxylate pendant arms on the aggregation state was thoroughly examined. Moreover, X-ray crystallographic studies of the Zr analogues revealed unique, bis(chelated) and trimetallic coordination modes that provided further insight into the role of carboxylate bridges in aggregation and catalysis. All five complexes were investigated as catalysts in the ring-opening polymerisation of *rac*-lactide.

## 2. Results and Discussion

### 2.1. Synthesis of Ti and Zr Clusters

The ethyl esters of a series of amino acids were used in the synthesis of ABP proligands (1–3) following procedures developed in our lab (Figure 2) [26,28]. To investigate their coordination chemistry with Ti, each proligand was reacted with titanium isopropoxide. The addition of  $\text{Ti}(\text{O}^i\text{Pr})_4$  to a solution of 1 in dry THF, and subsequent addition of one equivalent of water per Ti resulted in the formation of 4 (Figure 3). Performing the reactions without the deliberate addition of water leads to a mixture of products (of varying nuclearity) which were challenging to separate. Recrystallisation from a dichloromethane/acetonitrile solvent mixture afforded the tetrametallic cluster 4 as an orange solid in 52% yield. The coordination of Ti was confirmed through  $^1\text{H}$  NMR spectroscopy, which showed that the N-methylene hydrogens were diastereotopic through the formation of doublets ( $\text{CDCl}_3$  solvent,  $J = 12.4$  Hz) [25,26]. The absence of O-alkyl resonances ( $\text{CDCl}_3$  solvent,  $\delta = 4.27$  and 1.29 ppm) associated with the ethyl ester group on 1 indicated that the ester groups had been hydrolysed in situ. It is important to note that this result shows that the ester-protected ABP ligands can serve as an alternative route towards carboxylate-bridged Ti clusters, potentially offering more controlled coordination in comparison to the more reactive free carboxylates.

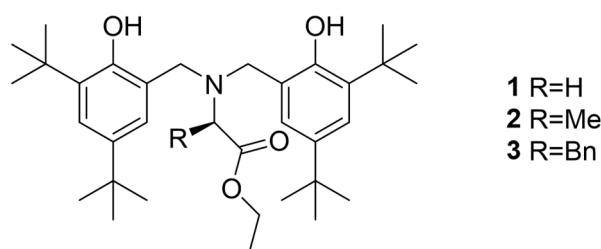


Figure 2. Structures of amino acid-derived ABP ligands 1–3.

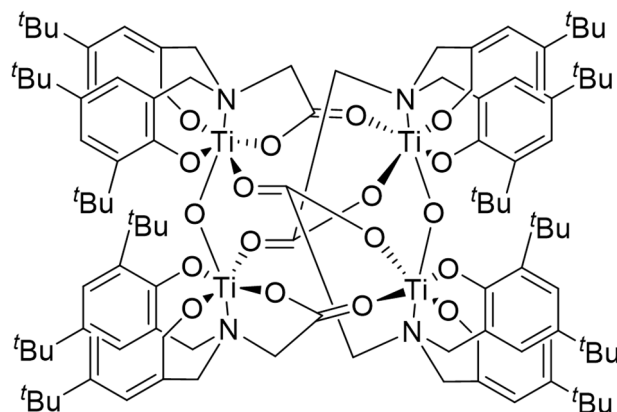
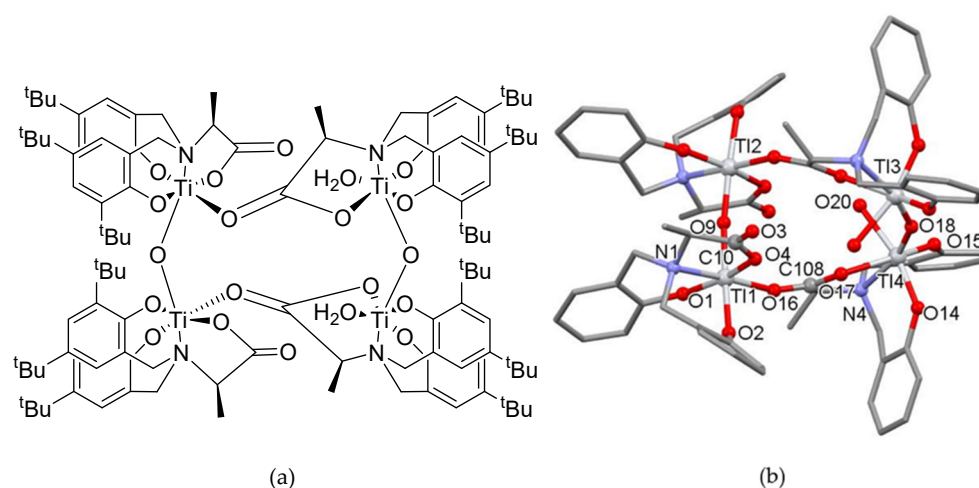


Figure 3. Tetrametallic Ti cluster 4.

The use of the alanine-derived ligand (2) led to the formation of a tetranuclear complex 5 in 47% yield. Single crystal X-ray diffraction (SCXRD) studies revealed a tetrametallic coordination mode, similar to 4; however, in this case only two of the carboxylate groups were involved in bridging between the Ti centres (Figure 4) [25]. The non-bridging carboxylate groups on Ti1 and Ti2 (Figure 4) show an average C=O bond length of 1.223(2) Å and C–O bond length of 1.296(1) Å, indicative of localised double and single bonds, respectively. This suggests that the carboxylates are bound as X-type ligands to the Ti centres Ti1 and Ti2. The Ti–O bonds, with an average length of 1.998(1) Å, are slightly elongated when compared to literature examples, which we attribute to the larger steric bulk around the metal centre [25,29,30]. The bridging carboxylates exhibit an average C–O bond length of 1.263(1) Å, indicating that the charge is fully delocalised, and these groups are acting as LX-type ligands. As there is no carboxylate bridging between Ti1 and Ti2, the sixth coordination site on Ti3 and Ti4 is occupied by water molecules. The two  $\mu$ -oxo-bridges present in the aggregate were found to be dissimilar, with the Ti1–O9–Ti2 angle close to linear at 173.4(2)°, while the Ti3–O18–Ti4 is significantly distorted at 148.6(2)°. The linear Ti1–O9–Ti2 bond showed a greater degree of Ti–O  $\pi$ -bonding than in the bent Ti3–O18–Ti4 bond due to Ti1 and Ti2 being more electron deficient metal centres [31]. This difference is also represented in the average Ti–N bond lengths at 2.252(2) Å and 2.295(1) Å for Ti1/2 and Ti3/4, respectively. The Ti–( $\mu$ -O) bond lengths are also different with an average length of 1.846(1) Å for Ti1/2–O9 and 1.823(1) Å for Ti3/4–O18. These values deviate slightly from those found in the literature for similar complexes. We ascribe this to repulsion between the *tert*-butyl groups on the phenol rings causing lengthening of the Ti–( $\mu$ -O) bonds, which leads to a reorientation of the structure, minimising this repulsion [32–35]. Complex 5 forms a partially closed tetrametallic cluster which indicates that increasing the steric bulk on the ABP pendant arm may limit the formation of the carboxylate bridges and prevent the core from completely closing, as in complex 4. This feature is promising from an ROP perspective, as an enhanced catalytic activity may arise from a more facile disaggregation of the Ti<sub>4</sub> cluster [25]. Despite not being fully closed, 5 was found to be stable towards air and moisture, allowing for convenient handling over several months.



**Figure 4.** Structure of Ti cluster **5** (a) and Crystal structure of **5** (b), Hydrogens, *tert*-butyl groups and solvent omitted for clarity. Selected bond lengths for **5** (Å): Ti1-O1 1.844(4), Ti1-O2 1.935(4), Ti1-O4 2.001(4), Ti1-O9 1.847(4), Ti1-O16 1.994(4), Ti1-N1 2.257(5), Ti4-O14 1.833(4), Ti4-O15 1.820(4), Ti4-O17 2.087(4), Ti4-O18 1.825(3), Ti4-O20 2.106(3), Ti4-N4 2.295(4), O3-C10 1.233(7), O4-C10 1.294(7), O16-C108 1.262(6), O17-C108 1.263(6). Selected bond angles for **5** (°): O1-Ti1-O2 92.7(2), O1-Ti1-O16 99.7(2), O1-Ti1-N1 84.7(2), O14-Ti4-O17 87.9(2), O14-Ti4-N4 87.2(2), Ti1-O9-Ti2 173.4(2), Ti3-O18-Ti4 148.6(2).

The series was further expanded using ligand **3** under identical conditions. After stirring for 16 h at room temperature, complex **6** formed as an orange powder with a yield of 55%. Single crystals, suitable for XRD, were grown via the vapour diffusion of acetonitrile into a chloroform solution of the complex. Remarkably, a binuclear complex was observed with the Ti centres linked by a single oxo-bridge (Figure 5). Complex **6** displayed a slightly distorted octahedral structure around each Ti atom, due to the bite angles of the tetradentate ligand restricting the perfect octahedral coordination geometry. Similar to **4** and **5**, the ester groups on the pendant arms have been hydrolysed, liberating the free carboxylate groups. The average C=O bond length of 1.244(5) Å and average C-O bond length of 1.315(3) Å indicate localised C=O and C-O bonds. The average Ti-O bond length for the carboxylates is 2.007(1) Å, further corroborating the X-type coordination of the carboxylate [29,30]. Unlike the tetrametallic structures **4** and **5**, in complex **6** the carboxylate moieties were not utilised in bonding between the Ti centres (Figure 5) [25]. Instead, a  $\mu$ -O bridge was formed, with Ti1-O6 bond length of 1.800(6) Å and Ti1-O6-Ti2 bond angle of 154.2(4)°, values that fall in line with literature examples [32,33]. The coordination spheres of the Ti centres are completed through the coordination of a water molecule. The lack of carboxylate bridges between the Ti centres is likely a result of the sterically demanding benzyl groups on **3** as this is in contrast to the complexes observed using the less sterically encumbered ligands (**1** and **2**).

From these results, it is evident that increasing the steric bulk of the ligand pendant arm has a significant impact on the formation of the clusters. The glycine derived ligand **1** (Figure 3) allowed for the formation of a fully closed tetrametallic cluster with four carboxylate bridges (**4**). Increasing the size of the R group on the ligand (Figure 2), from H to Me (**2**), resulted in a partially closed structure bridged by carboxylate moieties, while further increasing the substituent to Bn (**3**), eliminated the formation of the carboxylate bridges altogether. The delicate control over the size of the aggregate crucial in catalysis, as it has previously been reported that species with low nuclearity tend to have higher activity than aggregated species in the polymerisation of lactide [36].

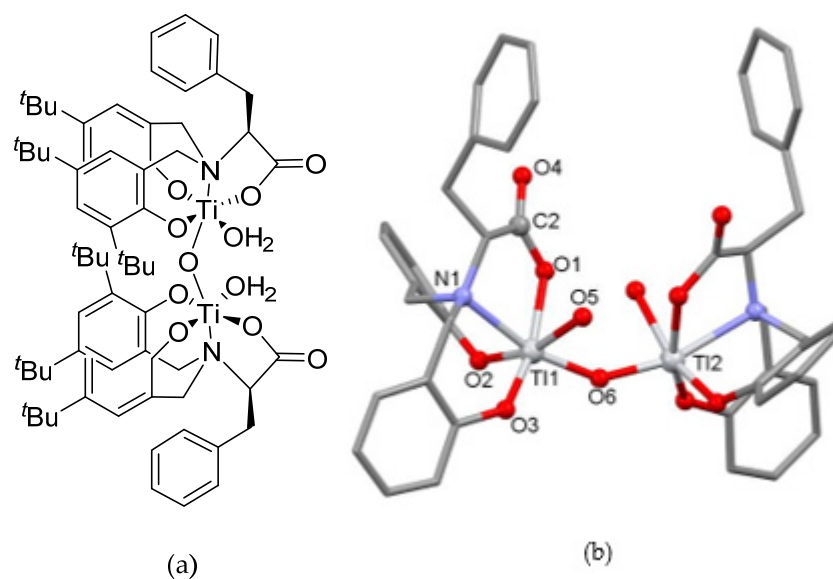


**Figure 5.** Ti cluster **6** (a), Crystal structure of **6** (b). Hydrogens, *tert*-butyl groups, and solvent omitted for clarity. Selected bond lengths for **6** (Å): Ti1-O1 2.010(7), Ti1-O2 1.872(6), Ti1-O3 1.822(6), Ti1-O5 2.145(6), Ti1-O6 1.827(6), Ti1-N1 2.289(8), Ti2-O6 1.806(6), O1-C2 1.30(1), O4-C2 1.259(13). Selected bond angles for **6** (°): O1-Ti1-O2 87.0(3), O1-Ti1-N1 75.6(3), O2-Ti1-O3 97.8(3), O2-Ti1-N1 86.9(3), Ti1-O6-Ti2 145.2(4).

The coordination of ABP ligand **1** to Zr was investigated using different metal precursors. The reaction of two equivalents of **1** with one equivalent of  $\text{Zr}(\text{O}^i\text{Pr})_4$ , afforded complex **7** with a yield of 13%, following recrystallisation from hexane at  $-34\text{ }^\circ\text{C}$ . Complexation was confirmed by the shifting of the aromatic C-H shifts associated with the ligand ( $\text{CDCl}_3$  solvent,  $\delta$  7.23 and 6.87 ppm) in the  $^1\text{H}$  NMR spectrum. X-ray studies revealed that **7** features two ABP ligands coordinated to a single Zr centre forming a distorted octahedral complex (Figure 6). This distortion is due to *ortho*-positioned *tert*-butyl groups sterically restricting the complex from forming a perfectly octahedral geometry. The average N-Zr-O bond angles of  $79.3(4)^\circ$  are within the expected range for bis(ABP) complexes [37]. The Zr-O and Zr-N bond distances fall in line with literature examples at an average of  $2.021(3)\text{ \AA}$  and  $2.398(3)\text{ \AA}$ , respectively [37–40]. Bischelated Zr complexes, similar to **7**, have previously been reported with amine bis and tris(phenolate) ligands, which feature relatively small steric bulk on the phenolate groups or on the Zr precursor [6,37,41,42]. Various bischelated Zr complexes have been reported in the literature, but to the best of our knowledge **7** is the first example of a bis(ABP) Zr complex, where the potentially coordinating ligand pendant arm remains unbound [37,39,40,42]. Surprisingly, it was also revealed that the complex now contains a propyl ester group. This presumably arises from hydrolysis of the ethyl ester and replacement by one of the displaced propoxides from the Zr precursor. An unbound ester group highlights the potential for post-synthetic modifications of the complex. When exposed to air and moisture, **7** proved to be robust, remaining unchanged over several months.

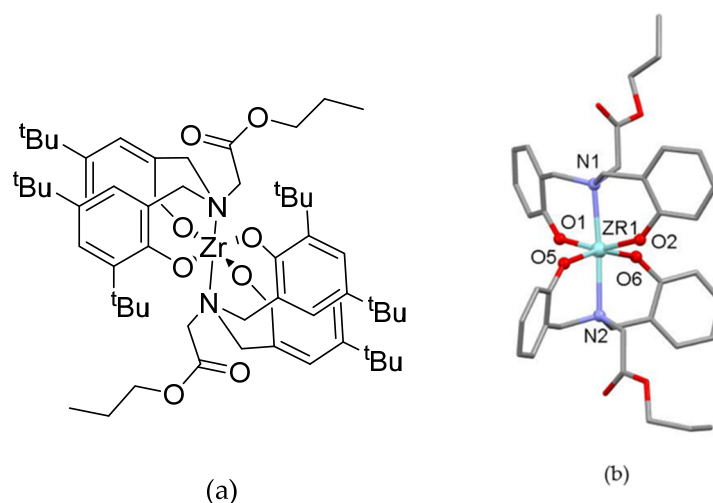


**Figure 6.** Zr bis(ABP) **7** (a), Crystal structure of **7** (b). Ligand structure represented by stick and Zr and atoms bound to Zr represented by ball and stick. Hydrogens and solvent omitted for clarity. Selected bond lengths for **7** (Å): Zr1-O1 2.032(3), Zr1-O2 2.030(3), Zr1-O5 2.009(3), Zr1-O6 2.013(3), Zr1-N1 2.396(3), Zr1-N2 2.398(3). Selected bond angles for **7** (°): O1-Zr1-N1 78.9(1), O2-Zr1-N1 80.0(1), N1-Zr1-N2 175.7(1).

Interestingly, using either the alanine- or phenylalanine-derived proligands (**2** and **3**), in combination with  $Zr(O^iPr)_4$ , under identical conditions did not result in the complexation of the ligand. This indicated that the sterically more demanding substituents on the pendant arm may completely inhibit the formation of further bis(chelated) Zr complexes. Literature examples corroborate this by showing that bulkier moieties on the pendant arm increase the Zr-N and Zr-O bond lengths and consequently weaken the coordination through steric hindrance [37]. Analysis of the structure of **7** shows that the methylene  $CH_2$  is in close proximity to the *ortho*-positioned *tert*-butyl groups on the opposing ligand (Figure S17); therefore, we anticipate that the substitution of H to Me or Bn would result in significant steric strain [37].

Reaction of **1** was also carried out with an alternative Zr precursor,  $Zr(O^tBu)_4$ , at 50 °C for five hours. Complex **8** was obtained as a white powder after recrystallisation from dichloromethane/methanol with a high yield of 56%. Complexation was confirmed by the shifting and increase in number of aromatic C-H resonances, associated with the ligand ( $CDCl_3$  solvent,  $\delta$  7.23 and 6.87 ppm), in the  $^1H$  NMR spectra. Single crystals, suitable for a SCXRD, were grown via vapour diffusion of chloroform/methanol. This study revealed the formation of a trimetallic species **8** with an unprecedented coordination mode. The metal centres were not bridged by the carboxylate groups as in **4** and **5**, instead the three Zr centres were held together via four  $\mu$ -oxo-bridges (Figure 7). Two different sets of oxo-bridges were observed: both the single and double oxo-bridges are within their expected bond lengths at 1.973(5) Å and 2.163(7) Å, respectively [21,43–45]. The Ti-O-Ti bond angles for the double oxo-bridge are narrower than the literature examples at 111.56(6)°, due to the shape of the overall structure forcing Zr1 and Zr3, closer together [43]. To the best of our knowledge, complex **8** is the first example of a trimetallic Zr cluster with amine bis/tris(phenolate) ligands where the Zr centres are bridged by only oxo-bridges [23,43,44,46]. The ester groups were not hydrolysed during the synthesis. The structure also showed that two of the Zr centres bonded by the double oxo-bridge were heptavalent, displaying distorted pentagonal bipyramidal geometries. The third Zr centre featuring two single oxo bridges formed a distorted octahedral structure. The Zr-N bond lengths are longer for Zr2 at 2.518(4) Å, suggesting that this metal centre is more electron rich than Zr1 and Zr3 at an average of 2.494(1) Å. All the Zr-N bonds are within the expected ranges [12,41].

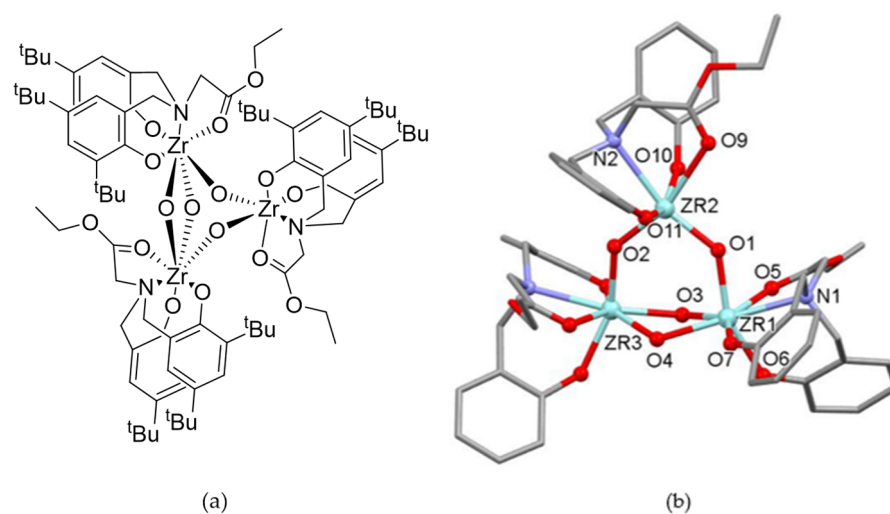


**Figure 7.** Structure of trimetallic Zr cluster **8** (a) and crystal structure of **8** (b). Ligand structure represented by stick and Zr and atoms bound to Zr shown by ball and stick. Hydrogens, *tert*-butyl groups, and solvent omitted for Selected bond lengths for **8** (Å): Zr1-O1 2.033(4), Zr1-O3 2.192(4), Zr1-O4 2.152(4), Zr1-O5 2.301(4), Zr1-O6 2.083(4), Zr1-O7 2.017(4), Zr1-N1 2.495(4), Zr2-O1 1.961(4), Zr2-O9 2.458(4), Zr2-O10 2.025(4), Zr2-O11 1.988(4), Zr2-O11 1.988(4), Zr2-N2 2.518(4). Selected bond angles for **8** (°): O1-Zr1-O3 93.0(2), O1-Zr1-O4 96.8(1), O1-Zr1-O5 82.5(1), O3-Zr1-O4 63.9(1), O9-Zr2-O10 76.0(2), O9-Zr2-N2 67.73(13), O9-Zr2-O11 83.8(1), Zr1-O1-Zr2 135.0(2), Zr1-O3-Zr3 111.4(2), Zr1-O4-Zr3 111.7(2).

## 2.2. Catalytic Activity in the ROP of *rac*-Lactide

Complexes **4–8** were trialled as catalysts in the ring-opening polymerisation of *rac*-lactide in the presence of benzyl-alcohol co-initiator (Table 1). The polymerisations were carried out under N<sub>2</sub> in sealed vials using 1 mol% catalyst loading at 130 °C for 24 h in toluene solvent [6,18,43]. First, the activity of the polymetallic Ti clusters was investigated: the bimetallic complex **6** achieved the highest conversion, reaching 73% (Table 1, entry 3), compared to 30% and 40% for the tetrametallic analogues **4** and **5**, respectively (entries 1 and 2). We attribute the variances to the different structures of each catalyst. While the tetramers' active site is shielded by significant steric bulk, in **6** the metal centre can be accessed more readily through the disassociation of the water ligand. Kinetic studies were carried out using complexes **5** and **6** revealing a linear reaction profile, with a rate of conversion of  $k_{obs} = 3.19 \times 10^{-2} \text{ h}^{-1}$  for **5** and  $k_{obs} = 1.51 \times 10^{-2} \text{ h}^{-1}$  for **6** (Figure 8). The higher reaction rate of **5** is surprising, considering that lower overall conversion was achieved in comparison to **6**; however, catalyst degradation in the later stages of the polymerisation may be responsible for this. The presence of *ortho*-positioned *tert*-butyl groups on the phenolate rings have been reported to decrease ROP activity, which may have contributed to the relatively low rates of conversion using catalysts **4–6** [47,48]. Complex **6** demonstrated no significant control on the tacticity of the polymer formed, providing atactic PLA chains with  $P_1$  values of 0.54 (Table 1, entry 5). The high-reaction temperatures and long-reaction times potentially facilitated epimerisation and transesterification side reactions [1,49]. When the temperature was decreased to 100 °C, the conversion dropped dramatically from 73% to 10% (Table 1, entry 6) using catalyst **6**. Size exclusion chromatography analysis of the PLA samples obtained using catalyst **6** showed average molecular weights of 3200–5800 Da, which fall well below the theoretical values of 22,000–25,000 Da. The accurate average molecular weights could not be determined using **4** and **5**, due to the polymers not precipitating in acidified methanol, suggesting that low-molecular-weight oligomers were formed. This can be attributed to the high temperatures and long reaction times applied, leading to significant transesterification reactions [1,49]. Analysis of the <sup>1</sup>H NMR spectra of polymer samples shows that both benzyl (CDCl<sub>3</sub> solvent,  $\delta$  7.36–7.31 ppm) and methoxy (CDCl<sub>3</sub> solvent,  $\delta$  3.76 ppm) end groups are present (Figure S19), originating

from the BnOH co-initiator and the MeOH used during purification. The polymerisation was found not to proceed in the absence of benzyl alcohol (Table S2, entries 1, 3 and 5), which was expected, as the catalyst structures do not contain a labile initiator to instigate the polymerisation. It is theorised that the carboxylate groups disassociate to allow for the coordination of the alkoxide.

**Table 1.** *rac*-lactide polymerisation data for complexes 4–8.

Entry	Cat.	[M]:[LA]	T (°C)	Time (h)	Conversion (%) <sup>b</sup>	P <sub>i</sub> <sup>c</sup>	M <sub>n(calcd)</sub> <sup>d</sup>	M <sub>n(obs)</sub>	<i>D</i>
1 <sup>a</sup>	4	1:100	130	24	31	-	4600	-	-
2 <sup>a</sup>	5	1:100	130	24	41	-	6000	-	-
3 <sup>a</sup>	6	1:100	130	24	73	-	10,600	-	-
4	6	1:200	130	48	88	0.51	22,900	3200	1.2
5	6	1:200	130	48	91	0.54	25,400	5800	1.3
6 <sup>a</sup>	6	1:100	100	24	10	-	1600	-	-
7 <sup>a</sup>	7	1:100	130	24	94	-	13,700	-	-
8 <sup>a</sup>	7	1:100	100	48	94	0.59	13,700	-	-
9	7	1:200	100	48	97	-	27,200	5000	1.5
10	8	1:100	130	24	95	0.54	14,000	4200	1.4
11	8	1:100	100	24	93	0.55	13,500	4200	1.2
12	8	1:200	100	48	96	0.62	26,900	10,800	1.3

Conditions [M]:[BnOH] = 1:2, [M] = 0.01 M, toluene. <sup>a</sup> Precipitation of polymer samples unsuccessful, due to the formation of short polymer chains. <sup>b</sup> Calculated from <sup>1</sup>H NMR analysis of the integration of the lactide and poly(lactic acid) resonances in the methylene region (Figure S18). <sup>c</sup> Determined using homonuclear decoupled <sup>1</sup>H NMR spectroscopy. <sup>d</sup> Calculated as  $M_{n(calcd)} = (([LA]/[M]) \times \text{conversion} \times MW_{LA}) + (M_{WEnd\ groups})$ .

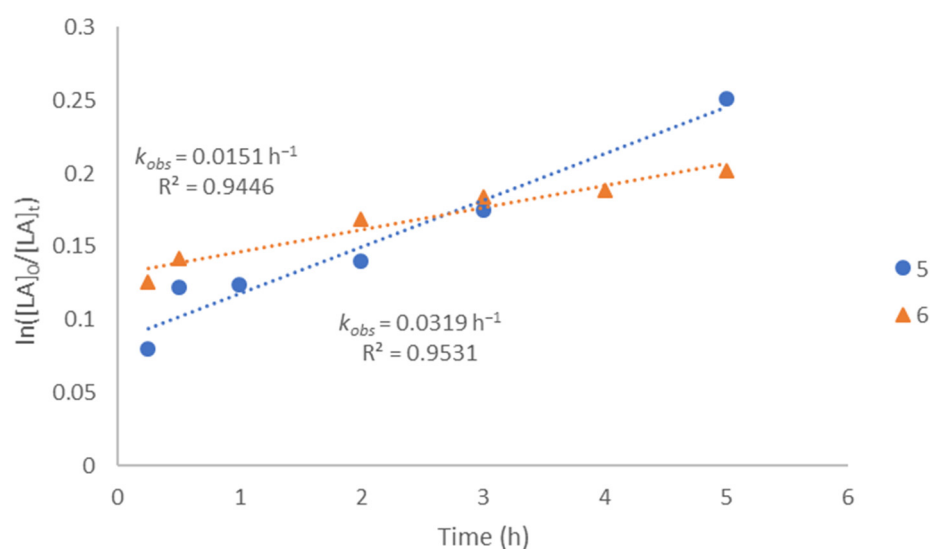


**Figure 8.** Kinetic plot for ROP of *rac*-lactide using complexes 5 and 6. Conditions: 100[LA]:[M], [LA] = 1 mol/L, BnOH = 2 μL, 130 °C.

The reported activity values using bis(chelated) Zr clusters with ABP or salen ligands in the literature are highly varied. Complex 7 falls into the category of highly active catalysts, achieving 94% conversion at 130 °C ( $k_{obs} = 0.181 \text{ h}^{-1}$ , Figure 9) after 24 h (Table 1, entry 7) [6,37,39,42,50,51]. When the reaction temperature was decreased to 100 °C, the conversion dropped to 68% (Table S2, entry 8). The rate of polymerisation is slower than that reported for similar homoleptic Zr complexes in solution [6,49,50], but this is somewhat expected for ligands with the large steric bulk of the two *ortho*-positioned *tert*-butyl groups on the phenolate rings [47,48]. Due to the relatively harsh conditions utilised in the polymerisation (100 °C, 48 h), complex 7 was found to have limited stereocontrol over the polymerisation, affording atactic PLA ( $P_i = 0.59$ , Table 1, entry 8). Analysis of the

polymers was challenging due to limited precipitation during the work-up. PLA samples isolated for GPC analysis showed limited control, with molecular weights (5000 Da, Table 1, entry 9) well below the theoretical values (of 27,200 Da, Table 1, entry 9) and a broad dispersity of molecular weights ( $D = 1.51$ ).

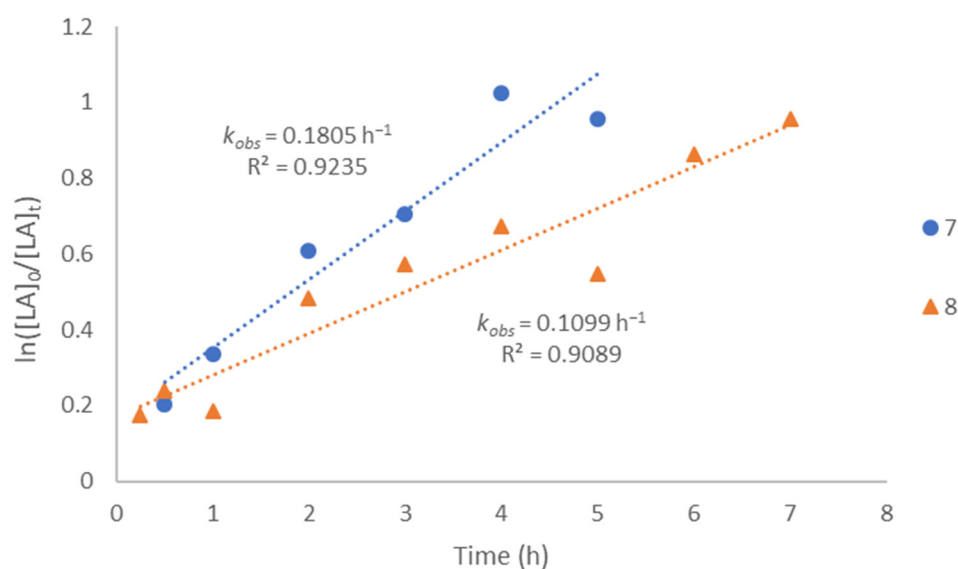


**Figure 9.** Kinetic plot for the ROP of *rac*-lactide using complexes 7 and 8. 100[LA]:[M], [LA] = 1 mol/L, BnOH = 2  $\mu$ L, 130  $^{\circ}$ C.

Trinuclear Zr complex 8 showed moderate rate of conversion ( $k_{obs} = 0.1099 \text{ h}^{-1}$ , Figure 9) in *rac*-lactide ROP at 130  $^{\circ}$ C, reaching 95% conversion in 24 h (Table 1, entry 8). Importantly, the reaction temperature using 8 could be reduced to 100  $^{\circ}$ C without significant loss of conversion after 24 h (93%; Table 1, entry 11). When the polymerisation was carried out at 100  $^{\circ}$ C, in the absence of benzyl alcohol, complex 8 achieved 91% conversion after 24 h (Table S2, entry 9). Complex 8 also exerted the highest stereocontrol with an isotactic bias of  $P_i = 0.62$ , which was attributed to the applied milder reaction conditions [49]. Due to the high activity at lower temperatures the formation of longer chain lengths (10,800 g/mol) was possible. However, the molecular weights were still significantly lower than the theoretical values (26,900 g/mol), suggesting that transesterification side-reactions also occurred [49].

### 3. Materials and Methods

#### 3.1. General Considerations

Starting materials were used as received from Merck, Acros Organics, Fischer Scientific and Alfa Aesar. Dry solvents were purified by a MBRAUN-800 SPS and stored over 4  $\text{\AA}$  molecular sieves under a dry nitrogen atmosphere. All NMR spectra were collected on a Bruker AVIII 300 MHz spectrometer at 298 K at Heriot-Watt University or on a Bruker AVIII 800 MHz spectrometer at 298 K at the University of Edinburgh. All mass spectrometry data was collected on a Bruker micrOTOF spectrometer at the University of Edinburgh. Elemental analyses were performed on an Exeter CE-440 Elemental Analyser. Air- and moisture-sensitive reactions were carried out using standard Schlenk techniques or an MBRAUN UNilab Plus glovebox with a  $\text{N}_2$  atmosphere. *D,L*-lactide was purified by triple sublimation prior to use. The tacticity of the collected polymers was determined using homonuclear decoupled  $^1\text{H}$  NMR spectroscopy and the method proposed by Coates and Ovitv (Figure S20) [11]. The Size Exclusion Chromatography analysis of polymers was carried using a Shimadzu High Performance Liquid Chromatograph fitted with a 7.5 mm internal diameter Agilent GPC column. The detector used was a Shimadzu RID-20A. HPLC grade tetrahydrofuran (THF, 99.8%, Acros Organics, Geel, Belgium) was utilized as the

eluent with flow rate of 1 mL/min with an oven temperature of 35 °C. The measurement was calibrated against 10 polystyrene standards in the range of 162–364,000 g/mol and corrected using the Mark–Houwink parameters, PLA ( $K = 0.0549$ ,  $\alpha = 0.639$ ) and PS ( $K = 0.0125$ ,  $\alpha = 0.717$ ) [52]. Proligands 1–3 were synthesised following literature protocols [26,28]. See supporting information for  $^1\text{H}$  and  $^{13}\text{C}$  NMR spectra.

### 3.2. General Procedure for the Synthesis of Ti ABP Complexes 4–6

An ABP proligand 1, 2 or 3 (0.5 mmol) was dissolved in dry THF (8 mL) in a nitrogen-filled Schlenk flask. To this solution, titanium isopropoxide (0.14 g, 15 mL, 0.5 mmol) was added dropwise. The yellow/green solution was stirred for 2 h at ambient temperature. Then, water (36  $\mu\text{L}$ , 2 mmol) was added and the reaction mixture was stirred for a further 16 h at ambient temperature. The volatiles were removed in vacuo. The obtained orange powder was purified via recrystallisation from dichloromethane/acetonitrile.

#### 3.2.1. Data for 4

Yield = 0.15 g, (52.4%).  $^1\text{H}$  NMR (300 MHz,  $\text{CDCl}_3$ , 25 °C)  $\delta$  7.29 (d,  $J = 2.3$  Hz, 4H, ArH), 7.21 (d,  $J = 2.3$  Hz, 4H, ArH), 6.85 (d,  $J = 2.3$  Hz, 4H, ArH), 6.74 (d,  $J = 2.3$  Hz, 4H, ArH), 3.56 (d,  $J = 12.6$  Hz, 4H,  $\text{NCH}_2$ ), 3.36 (d,  $J = 12.5$  Hz, 4H,  $\text{NCH}_2$ ), 3.13 (q,  $J = 22.5$  Hz, 8H,  $\text{CH}_2\text{COO}$ ), 2.74 (d,  $J = 12.7$  Hz, 4H,  $\text{NCH}_2$ ), 2.60 (d,  $J = 12.8$  Hz, 4H,  $\text{NCH}_2$ ), 1.57 (s, 36 H,  $\text{CCH}_3$ ), 1.48 (s, 36H,  $\text{CCH}_3$ ), 1.24 (s, 36H,  $\text{CCH}_3$ ), 1.23 (s, 36H,  $\text{CCH}_3$ ).  $^{13}\text{C}$  NMR (75.5 MHz,  $\text{CDCl}_3$ , 25 °C)  $\delta$  181.3, 162.5, 158.6, 141.9, 141.4, 136.2, 135.5, 126.2, 125.2, 124.9, 123.8, 123.6, 66.2, 62.6, 61.0, 35.4, 35.1, 34.5, 34.4, 32.1, 31.8, 31.2, 30.9. HRMS (ESI):  $m/z$   $[\text{M}+\text{H}]^+$  found 2258.16010,  $[\text{M}+\text{H}]^+$  calculated 2258.15963. Elemental analysis calculated for  $\text{C}_{128}\text{H}_{184}\text{N}_4\text{O}_{18}\text{Ti}_4$ : C, 68.08; H, 8.21; N, 2.48, Found: C, 67.57; H, 8.07; N, 2.30.

#### 3.2.2. Data for 5

Yield = 0.14 g, (47.2%).  $^1\text{H}$  NMR (300 MHz,  $\text{CDCl}_3$ , 25 °C)  $\delta$  7.30 (d,  $J = 2.4$  Hz, 4H, ArH), 7.17 (bs, 4H, ArH) 7.00 (d,  $J = 2.3$  Hz, 4H, ArH), 6.97 (d,  $J = 2.2$  Hz, 4H, ArH), 4.76–4.71 (m, 12H,  $\text{NCH}_2$ ), 3.95 (q,  $J = 6.7$  Hz, 4H,  $\text{CHCOO}$ ), 3.68–3.41 (m, 8H,  $\text{NCH}_2$ ), 3.22–3.00 (m, 4H  $\text{NCH}_2$ ), 2.58 (bs, 24H,  $\text{H}_2\text{O}$ ), 1.58 (bs, 36H,  $\text{CCH}_3$ ), 1.52–1.39 (m,  $J = 6.8$  Hz, 47H,  $\text{CCH}_3$ ), 1.29 (s, 36H,  $\text{CCH}_3$ ), 1.22 (s, 36 H,  $\text{CCH}_3$ ).  $^{13}\text{C}$  NMR (75.5 MHz,  $\text{CDCl}_3$ , 25 °C)  $\delta$  159.2, 143.1, 125.5, 125.0, 124.8, 35.4, 35.0, 34.5, 34.4, 31.8, 31.7, 31.0, 30.7, 30.1.  $^{13}\text{C}$  NMR (75.5 MHz,  $\text{C}_6\text{D}_6$ , 25 °C)  $\delta$  177.8, 163.4, 159.5, 142.7, 142.1, 136.7, 135.3, 126.4, 125.8, 125.3, 124.7, 124.3, 123.1, 77.7, 64.5, 35.8, 35.2, 34.6, 34.4, 32.0, 31.9, 31.3, 30.4, 9.8. HRMS (ESI):  $m/z$   $[\text{M}-2(\text{H}_2\text{O})+\text{Na}]^+$  found 2337.20562,  $[\text{M}-2(\text{H}_2\text{O})+\text{Na}]^+$  calculated 2337.21017. Elemental analysis calculated for  $\text{C}_{132}\text{H}_{196}\text{N}_4\text{O}_{20}\text{Ti}_4(\text{CHCl}_3)$ : C, 64.68; H, 8.04; N, 2.27, Found: C, 64.57; H, 8.36; N, 2.40.

#### 3.2.3. Data for 6

Yield = 0.18 g, (55.2%)  $^1\text{H}$  NMR (300 MHz,  $\text{CDCl}_3$ , 25 °C)  $\delta$  7.40–7.27 (m, 12H, ArH), 7.25–7.20 (m, 1H, ArH), 7.03 (s, 2H, ArH), 6.72 (s, 2H, ArH), 4.06 (s, 4H,  $\text{NCH}_2$ ), 3.83–3.72 (m, 3H), 3.57 (d,  $J = 12.6$  Hz, 4H,  $\text{CHCH}_2\text{Ph}$ ) 3.44–3.30 (m, 5H,  $\text{NCH}_2$ ), 3.22–3.10 (m, 2H,  $\text{NCH}_2$ ), 1.67 (s, 18 H,  $\text{CCH}_3$ ), 1.42 (s, 18 H,  $\text{CCH}_3$ ), 1.30 (s, 18 H,  $\text{CCH}_3$ ), 1.24 (s, 18 H,  $\text{CCH}_3$ ).  $^{13}\text{C}$  NMR (75.5 MHz,  $\text{CDCl}_3$ , 25 °C)  $\delta$  159.0, 143.4, 139.6, 129.6, 129.5, 128.9, 128.5, 126.8, 125.2, 125.0, 124.6, 35.3, 35.2, 34.5, 34.5, 31.8, 31.7, 31.1, 30.9, 30.2, 30.0, 29.8. HRMS (ESI):  $m/z$   $[\text{M}+\text{Na}]^+$  found 1367.6817,  $[\text{M}+\text{Na}]^+$  calculated 1367.8615. Elemental analysis calculated for  $\text{C}_{78}\text{H}_{108}\text{N}_2\text{O}_{11}\text{Ti}_2(\text{CHCl}_3)$ : C, 64.78; H, 7.50; N, 1.91, Found: C, 64.45; H, 7.96; N, 1.70.

### 3.3. Synthesis of Zr ABP Complexes

#### 3.3.1. Data for 7

Proligand 1 (2.16 g, 4 mmol) was dissolved in toluene (60 mL). To this, zirconium propoxide (1.3 g, 1.88 mL of 70 w.t.% in propan-1-ol, 4 mmol) was added dropwise. The reaction mixture was heated to reflux for 20 h, after this time the volatiles were removed

and the product was purified by recrystallisation in hexane at  $-34\text{ }^{\circ}\text{C}$ . Yield = 0.31 g, (13.1%)  $^1\text{H}$  NMR (300 MHz,  $\text{CDCl}_3$ ,  $25\text{ }^{\circ}\text{C}$ )  $\delta$  7.25 (d,  $J = 2.5\text{ Hz}$ , 2H, ArH), 7.09 (d,  $J = 2.4\text{ Hz}$ , 2H, ArH), 7.03 (d,  $J = 2.3\text{ Hz}$ , 2H, ArH), 6.91 (d,  $J = 2.36\text{ Hz}$ , 2H, ArH), 4.86 (d,  $J = 12.6\text{ Hz}$ , 2H,  $\text{NCH}_2$ ), 4.62 (d,  $J = 12.5\text{ Hz}$ , 2H,  $\text{NCH}_2$ ), 4.44 (m, 4H,  $\text{NCH}_2$ ), 4.12–4.00 (m, 2H,  $\text{CH}_2\text{COOEt}$ ), 3.92–3.83 (m, 2H,  $\text{CH}_2\text{COOEt}$ ), 3.65 (d,  $J = 17.6\text{ Hz}$ , 2H,  $\text{NCH}_2$ ), 3.28 (d,  $J = 17.6\text{ Hz}$ , 2H,  $\text{NCH}_2$ ), 1.41 (s, 18H,  $\text{CCH}_3$ ) 1.27 (s, 18H,  $\text{CCH}_3$ ), 1.23 (s, 18H,  $\text{CCH}_3$ ), 0.9 (s, 18H,  $\text{CCH}_3$ ), 0.84 (t,  $J = 7.4\text{ Hz}$ , 6H,  $\text{CH}_2\text{CH}_3$ ).  $^{13}\text{C}$  NMR (75.5 MHz,  $\text{CDCl}_3$ ,  $25\text{ }^{\circ}\text{C}$ )  $\delta$  168.4, 158.5, 157.7, 140.2, 139.8, 135.6, 134.7, 125.6, 124.7, 124.4, 124.2, 123.1, 121.5, 65.9, 58.4, 58.0, 46.8, 34.9, 34.4, 34.3, 34.1, 31.8, 31.8, 31.1, 30.2, 29.8, 22.0, 10.5. HRMS (ESI):  $m/z$   $[\text{M}+\text{H}]^+$  found 1193.70470,  $[\text{M}+\text{H}]^+$  calculated 1193.70690. Elemental analysis calculated for  $\text{C}_{70}\text{H}_{106}\text{N}_2\text{O}_8\text{Zr}$ : C, 70.73; H, 8.94; N, 2.34, Found: C, 69.97; H, 8.88; N, 2.24.

### 3.3.2. Data for 8

Proligand **1** (0.27 g, 0.5 mmol) was placed into a nitrogen-filled Schlenk flask and dissolved in dry THF (8 mL). Zirconium *tert*-butoxide (0.19 g, 0.20 mL, 0.5 mmol) was added dropwise. The reaction mixture was heated to  $50\text{ }^{\circ}\text{C}$  for 5 h. The reaction was left to cool to room temperature and stirred for a further 16 h. The volatiles were removed by vacuum and the resulting solid was recrystallised in DCM/acetonitrile. Yield = 0.18 g (56.6%).  $^1\text{H}$  NMR (300 MHz,  $\text{CDCl}_3$ ,  $25\text{ }^{\circ}\text{C}$ )  $\delta$  7.20 (d,  $J = 2.3\text{ Hz}$ , 1H, ArH), 7.16 (d,  $J = 2.4\text{ Hz}$ , 1H, ArH), 7.15–7.10 (m, 3H, ArH), 7.01 (d,  $J = 2.3\text{ Hz}$ , 1H, ArH) 6.86 (d,  $J = 2.3\text{ Hz}$ , 1H, ArH), 6.82–6.77 (m, 4H, ArH), 6.72 (d,  $J = 2.1\text{ Hz}$ , 1H, ArH), 5.50 (d,  $J = 11.9\text{ Hz}$ , 2H,  $\text{NCH}_2$ ), 5.37 (m, 2H,  $\text{CH}_2\text{COOEt}$ ), 5.14 (d,  $J = 10.9\text{ Hz}$ , 1H,  $\text{NCH}_2$ ), 4.80 (d,  $J = 12.2\text{ Hz}$ , 1H,  $\text{NCH}_2$ ), 4.48 (d,  $J = 11.3\text{ Hz}$ , 1H,  $\text{NCH}_2$ ), 4.25 (d,  $J = 14.3\text{ Hz}$ , 1H,  $\text{NCH}_2$ ), 4.18–4.06 (m, 1H), 4.05–3.95 (m, 2H,  $\text{CH}_2\text{COOEt}$ ), 3.88 (d,  $J = 12.4\text{ Hz}$ , 1H,  $\text{NCH}_2$ ), 3.76–3.63 (m, 2H), 3.60–3.42 (m, 2H), 3.38–3.08 (m, 8H), 2.85 (d,  $J = 17.3\text{ Hz}$ , 1H,  $\text{NCH}_2$ ), 2.53 (t,  $J = 11.7\text{ Hz}$ , 2H,  $\text{CH}_2\text{COOEt}$ ), 1.51 (d,  $J = 4.8\text{ Hz}$ , 18H,  $\text{CCH}_3$ ), 1.39 (d,  $J = 7.1\text{ Hz}$ , 18H,  $\text{CCH}_3$ ), 1.29 (m, 22H,  $\text{CCH}_3$ ), 1.25 (s, 18H,  $\text{CCH}_3$ ), 1.23–1.19 (m, 25H,  $\text{CCH}_3$ ), 1.03 (t,  $J = 7.2\text{ Hz}$ , 3H,  $\text{CH}_2\text{CH}_3$ ), 0.84 (t,  $J = 7.2\text{ Hz}$ , 3H,  $\text{CH}_2\text{CH}_3$ ), 0.46 (t,  $J = 7.1\text{ Hz}$ , 2H,  $\text{CH}_2\text{CH}_3$ ).  $^{13}\text{C}$  NMR (75.5 MHz,  $\text{CDCl}_3$ ,  $25\text{ }^{\circ}\text{C}$ )  $\delta$  177.2, 177.0, 176.3, 161.3, 160.8, 160.0, 159.4, 158.6, 158.3, 138.1, 137.8, 137.7, 137.5, 137.4, 137.3, 136.9, 136.4, 136.3, 136.0, 125.4, 124.5, 124.4, 123.9, 123.8, 123.7, 123.5, 123.4, 123.1, 123.0, 122.8, 122.6, 122.4, 64.2, 63.7, 63.5, 63.2, 62.8, 62.6, 62.0, 61.6, 61.4, 60.5, 60.2, 35.0, 34.9, 34.8, 34.6, 34.5, 34.4, 34.0, 33.9, 33.9, 33.9, 32.0, 31.8, 31.8, 31.7, 30.7, 30.5, 30.0, 29.7, 29.5, 29.2, 13.6, 13.4, 12.8. HRMS (ESI):  $m/z$   $[\text{M}]^+$  found 1945.8341,  $[\text{M}]^+$  calculated 1945.8387. Elemental analysis calculated for  $\text{C}_{102}\text{H}_{153}\text{N}_3\text{O}_{16}\text{Zr}_3$ : C, 62.79; H, 7.90; N, 2.15, Found: C, 61.87; H, 7.62; N, 1.78.

### 3.4. General Procedure for the Polymerisation of *rac*-Lactide

*D,L*-lactide (0.14 g, 1 mmol), the catalyst (0.01 mmol) and benzyl alcohol (5  $\mu\text{L}$ , 0.05 mmol) were dissolved in dry toluene (1 mL) under  $\text{N}_2$ . The sealed vial was heated to  $130\text{ }^{\circ}\text{C}$  for the appropriate reaction time. An aliquot was taken for  $^1\text{H}$  NMR analysis to determine conversion. The bulk was quenched with ice-cold acidified methanol. The precipitate was filtered and dried under vacuum until constant weight was reached.

### 3.5. Crystallography

All crystal structures were collected on a Bruker D8 Venture, with  $\text{Mo-K}\alpha$  ( $\lambda = 0.7107\text{ \AA}$ ) or with a  $\text{Cu-K}\alpha$  ( $\lambda = 1.5418\text{ \AA}$ ) source at 100 K, cooled with an Oxford Cryosystems Cryostream. The structures were solved by intrinsic phasing SHELXT and refined by full-matrix least-squares on  $F^2$  using SHELXL interfaced through Olex2 [53–55]. Molecular graphics for all structures were generated using Mercury [56]. See supporting information for crystallographic and refinement details. The supplementary crystallographic data can be found free of charge on the joint Cambridge Crystallographic Data Centre and Fachinformationszentrum Karlsruhe Access Structures service. Deposition numbers 2074322 (5), 2074525 (6), 2074533 (7) and 2074596 (8).

#### 4. Conclusions

To conclude, a series of five polymetallic Ti and Zr clusters were synthesised and fully characterised using amino acid ethyl ester-derived bis(phenolate) ligands. X-ray crystallographic studies of the aggregates revealed a varying number of metal centres can be bridged by carboxylate groups and oxygen atoms. The size of aggregates formed was found to be easily fine-tuned by modifying the steric bulk on the ABP ligand's pendant arm. The Ti complex of the glycine-derived ABP ligand formed a tetranuclear species with four carboxylate bridges between the metal centres. The alanine-derived ligand also formed a tetramer; however, the increased steric bulk impeded the number of possible carboxylate bridges, leading to two bridging and two non-bridging carboxylate groups. The most sterically demanding phenylalanine-derived ABP ligand afforded binuclear Ti species featuring a single  $\mu$ -oxo-bridge. Using the glycine-derived ABP ligand and different Zr precursors, two novel Zr complexes were synthesised with unique structures. Firstly, a bischelated Zr complex formed, featuring an uncoordinated binding site on the pendant arm of the ligand. A trimetallic Zr cluster, bridged entirely by oxo-bridges, was also formed. Complexes were found to be tolerant to air and moisture and stable in solution for an extended period. All complexes were applied as catalysts for the ROP of *rac*-lactide. The Ti tetramers were shown to have a limited rate of polymerisation, while the binuclear Ti complex exerted relatively faster rates. Two Zr complexes were also shown to be effective catalysts in the ROP of *rac*-lactide, achieving a high rate of polymerisation, with a trimetallic derivative providing enhanced control over the PLA tacticity. Further investigation into the mechanism of the catalysts is ongoing.

**Supplementary Materials:** The following are available online at <https://www.mdpi.com/article/10.3390/catal11050551/s1>, Supporting information file. Figure S1:  $^1\text{H}$  NMR spectrum of complex 4 (300 MHz,  $\text{CDCl}_3$ , 25 °C), Figure S2:  $^{13}\text{C}$  NMR spectrum of complex 4 (75.5 MHz,  $\text{CDCl}_3$ , at 25 °C), Figure S3:  $^1\text{H}$  NMR spectrum of complex 5 (300 MHz,  $\text{CDCl}_3$ , 25 °C), Figure S4:  $^{13}\text{C}$  NMR spectrum of complex 5 (75.5 MHz,  $\text{CDCl}_3$ , at 25 °C), Figure S5:  $^{13}\text{C}$  NMR spectrum of complex 5 (75.5 MHz,  $\text{C}_6\text{D}_6$ , at 25 °C), Figure S6:  $^1\text{H}$  NMR spectrum of complex 6 (300 MHz,  $\text{CDCl}_3$ , 25 °C), Figure S7:  $^{13}\text{C}$  NMR spectrum of complex 6 (75.5 MHz,  $\text{CDCl}_3$ , at 25 °C), Figure S8:  $^1\text{H}$  NMR spectrum of complex 7 (300 MHz,  $\text{CDCl}_3$ , 25 °C), Figure S9:  $^{13}\text{C}$  NMR spectrum of complex 7 (75.5 MHz,  $\text{CDCl}_3$ , at 25 °C), Figure S10:  $^1\text{H}$  NMR spectrum of complex 8 (300 MHz,  $\text{CDCl}_3$ , 25 °C), Figure S11:  $^{13}\text{C}$  NMR spectrum of complex 8 (75.5 MHz,  $\text{CDCl}_3$ , at 25 °C), Figure S12: HRMS data for complex 4, Figure S13: HRMS data for complex 5, Figure S14: HRMS data for complex 6, Figure S15: HRMS data for complex 7, Figure S16: HRMS data for complex 8, Figure S17: Crystal structure of 7, Figure S18:  $^1\text{H}$  NMR spectra of crude ROP reaction mixture (300 MHz,  $\text{CDCl}_3$ , at 25 °C), Figure S19:  $^1\text{H}$  NMR spectra of purified PLA sample (300 MHz,  $\text{CDCl}_3$ , at 25 °C), Figure S20: Example homonuclear decoupled  $^1\text{H}$  NMR spectra of purified PLA sample, Table S1: Crystallographic and refinement details for complexes 5–8, Table S2: Supplementary polymerisation data.

**Author Contributions:** Conceptualization, R.D.M.; methodology and investigation, D.T.J. and E.F.; analysis, G.M.R. and S.B.H.P.; writing—original draft preparation, D.T.J., E.F. and R.D.M.; writing—review and editing, D.T.J., E.F., R.D.M., S.B.H.P., G.M.R. and F.V.; supervision, R.D.M. and F.V.; funding acquisition, R.D.M. All authors have read and agreed to the published version of the manuscript.

**Funding:** This research was funded by EPSRC, grant numbers EP/N509474/1 and EP/S005781/1.

**Data Availability Statement:** The supplementary crystallographic data can be found free of charge on the joint Cambridge Crystallographic Data Centre and Fachinformationszentrum Karlsruhe Access Structures service. Deposition numbers 2074322 (5), 2074525 (6), 2074533 (7) and 2074596 (8).

**Acknowledgments:** The authors thank Juraj Bella and Lorna Murray at the University of Edinburgh for their assistance and access to the 800 MHz spectrometer; the authors would also like to thank Stephen M. Mansell for providing access to a glovebox.

**Conflicts of Interest:** The authors declare no conflict of interest. The funders had no role in the design of the study; in the collection, analyses, or interpretation of data; in the writing of the manuscript, or in the decision to publish the results.

## References

1. Sauer, A.; Kapelski, A.; Fliedel, C.; Dagorne, S.; Kol, M.; Okuda, J. Structurally well-defined group 4 metal complexes as initiators for the ring-opening polymerization of lactide monomers. *Dalton Trans.* **2013**, *42*, 9007–9023. [[CrossRef](#)]
2. Thomas, C.M. Stereocontrolled ring-opening polymerization of cyclic esters: Synthesis of new polyester microstructures. *Chem. Soc. Rev.* **2010**, *39*, 165–173. [[CrossRef](#)]
3. Darensbourg, D.J.; Karroonnirun, O. Ring-opening polymerization of lactides catalyzed by natural amino-acid based zinc catalysts. *Inorg. Chem.* **2010**, *49*, 2360–2371. [[CrossRef](#)]
4. Daneshmand, P.; Jiménez-Santiago, J.L.; Aragon-Alberti, M.; Schaper, F. Catalytic-Site-Mediated Chain-End Control in the Polymerization of *rac*-Lactide with Copper Iminopyrrolide Complexes. *Organometallics* **2018**, *37*, 1751–1759. [[CrossRef](#)]
5. Coates, G.W. Precise Control of Polyolefin Stereochemistry Using Single-Site Metal Catalysts. *Chem. Rev.* **2000**, *100*, 1223–1252. [[CrossRef](#)] [[PubMed](#)]
6. Hu, M.; Han, F.; Zhang, W.; Ma, W.; Deng, Q.; Song, W.; Yan, H.; Dong, G. Preparation of zirconium and hafnium complexes containing chiral N atoms from asymmetric tertiary amine ligands, and their catalytic properties for polymerization of *rac*-lactide. *Catal. Sci. Technol.* **2017**, *7*, 1394–1403. [[CrossRef](#)]
7. Chmura, A.J.; Davidson, M.G.; Frankis, C.J.; Jones, M.D.; Lunn, M.D. Highly active and stereoselective zirconium and hafnium alkoxide initiators for solvent-free ring-opening polymerization of *rac*-lactide. *Chem. Commun.* **2008**, *11*, 1293–1295. [[CrossRef](#)]
8. Chmura, A.J.; Chuck, C.J.; Davidson, M.G.; Jones, M.D.; Lunn, M.D.; Bull, S.D.; Mahon, M.F. A germanium alkoxide supported by a C<sub>3</sub>-symmetric ligand for the stereoselective synthesis of highly heterotactic polylactide under solvent-free conditions. *Angew. Chem. Int. Ed.* **2007**, *46*, 2280–2283. [[CrossRef](#)] [[PubMed](#)]
9. Spassky, N.; Wisniewski, M.; Pluta, C.; Borgne, A.L. Highly stereoelective polymerization of *rac*-(D,L)-lactide with a chiral schiff's base/aluminium alkoxide initiator. *Macromol. Chem. Phys.* **1996**, *197*, 2627–2637. [[CrossRef](#)]
10. Radano, C.P.; Baker, G.L.; Smith, M.R. Stereoselective Polymerization of a Racemic Monomer with a Racemic Catalyst: Direct Preparation of the Polylactic Acid Stereocomplex from Racemic Lactide. *J. Am. Chem. Soc.* **2000**, *122*, 1552–1553. [[CrossRef](#)]
11. Ovitt, T.M.; Coates, G.W. Stereochemistry of Lactide Polymerization with Chiral Catalysts: New Opportunities for Stereocontrol Using Polymer Exchange Mechanisms. *J. Am. Chem. Soc.* **2002**, *124*, 1316–1326. [[CrossRef](#)]
12. Chmura, A.J.; Davidson, M.G.; Jones, M.D.; Lunn, M.D.; Mahon, M.F.; Johnson, A.F.; Khunkamchoo, P.; Roberts, S.L.; Wong, S.S.F. Group 4 Complexes with Aminebisphenolate Ligands and Their Application for the Ring Opening Polymerization of Cyclic Esters. *Macromolecules* **2006**, *39*, 7250–7257. [[CrossRef](#)]
13. Nomura, N.; Ishii, R.; Akakura, M.; Aoi, K. Stereoselective Ring-Opening Polymerization of Racemic Lactide Using Aluminum-Achiral Ligand Complexes: Exploration of a Chain-End Control Mechanism. *J. Am. Chem. Soc.* **2002**, *124*, 5938–5939. [[CrossRef](#)] [[PubMed](#)]
14. Zelikoff, A.L.; Kopilov, J.; Goldberg, I.; Coates, G.W.; Kol, M. New facets of an old ligand: Titanium and zirconium complexes of phenylenediamine bis(phenolate) in lactide polymerisation catalysis. *Chem. Commun.* **2009**, 6804–6806. [[CrossRef](#)] [[PubMed](#)]
15. Kirk, S.M.; Kociok-Köhn, G.; Jones, M.D. Zirconium vs Aluminum Salalen Initiators for the Production of Biopolymers. *Organometallics* **2016**, *35*, 3837–3843. [[CrossRef](#)]
16. Arnold, P.L.; Buffet, J.C.; Blaudeck, R.P.; Sujecki, S.; Blake, A.J.; Wilson, C. C<sub>3</sub>-symmetric lanthanide tris(alkoxide) complexes formed by preferential complexation and their stereoselective polymerization of *rac*-lactide. *Angew. Chem. Int. Ed.* **2008**, *47*, 6033–6036. [[CrossRef](#)] [[PubMed](#)]
17. Jianming, R.; Anguo, X.; Hongwei, W.; Hailin, Y. Review—Recent development of ring-opening polymerization of cyclic esters using aluminum complexes. *Des. Monomers Polym.* **2013**, *17*, 345–355. [[CrossRef](#)]
18. Sun, Z.; Zhao, Y.; Santoro, O.; Elsegood, M.R.J.; Bedwell, E.V.; Zahra, K.; Walton, A.; Redshaw, C. Use of titanocalix[4]arenes in the ring opening polymerization of cyclic esters. *Catal. Sci. Technol.* **2020**, *10*, 1619–1639. [[CrossRef](#)]
19. Liu, Y.; Dawe, L.N.; Kozak, C.M. Bimetallic and trimetallic zinc amino-bis(phenolate) complexes for ring-opening polymerization of *rac*-lactide. *Dalton Trans.* **2019**, *48*, 13699–13710. [[CrossRef](#)]
20. Nie, K.; Fang, L.; Yao, Y.; Zhang, Y.; Shen, Q.; Wang, Y. Synthesis and characterization of amine-bridged bis(phenolate)lanthanide alkoxides and their application in the controlled polymerization of *rac*-lactide and *rac*-beta-butyrolactone. *Inorg. Chem.* **2012**, *51*, 11133–11143. [[CrossRef](#)]
21. Su, C.-K.; Chuang, H.-J.; Li, C.-Y.; Yu, C.-Y.; Ko, B.-T.; Chen, J.-D.; Chen, M.-J. Oxo-Bridged Bimetallic Group 4 Complexes Bearing Amine-Bis(benzotriazole phenolate) Derivatives as Bifunctional Catalysts for Ring-Opening Polymerization of Lactide and Copolymerization of Carbon Dioxide with Cyclohexene Oxide. *Organometallics* **2014**, *33*, 7091–7100. [[CrossRef](#)]
22. Degée', P.; Dubois, P.; Jérôme, R.; Jacobsen, S.; Fritz, H.-G. New catalysis for fast bulk ring-opening polymerization of lactide monomers. *Macromol. Symp.* **1999**, *144*, 289–302. [[CrossRef](#)]
23. Jeffery, B.J.; Whitelaw, E.L.; Garcia-Vivo, D.; Stewart, J.A.; Mahon, M.F.; Davidson, M.G.; Jones, M.D. Group 4 initiators for the stereoselective ROP of *rac*-beta-butyrolactone and its copolymerization with *rac*-lactide. *Chem. Commun.* **2011**, *47*, 12328–12330. [[CrossRef](#)]
24. Gendler, S.; Segal, S.; Goldberg, I.; Goldschmidt, Z.; Kol, M. Titanium and zirconium complexes of dianionic and trianionic amine-phenolate-type ligands in catalysis of lactide polymerization. *Inorg. Chem.* **2006**, *45*, 4783–4790. [[CrossRef](#)]
25. Cols, J.E.; Taylor, C.E.; Gagnon, K.J.; Teat, S.J.; McIntosh, R.D. Well-defined Ti<sub>4</sub> pre-catalysts for the ring-opening polymerisation of lactide. *Dalton Trans.* **2016**, *45*, 17729–17738. [[CrossRef](#)] [[PubMed](#)]

26. Cols, J.E.P.; Hill, V.G.; Williams, S.K.; McIntosh, R.D. Aggregated initiators: Defining their role in the ROP of rac-lactide. *Dalton Trans.* **2018**, *47*, 10626–10635. [[CrossRef](#)]
27. Redshaw, C.; Tang, Y. Tridentate ligands and beyond in group IV metal  $\alpha$ -olefin homo-/co-polymerization catalysis. *Chem. Soc. Rev.* **2012**, *41*, 4484–4510. [[CrossRef](#)]
28. Fazekas, E.; Jenkins, D.T.; Forbes, A.A.; Gallagher, B.; Rosair, G.M.; McIntosh, R.D. Amino acid-derived bisphenolate palladium complexes as C-C coupling catalysts. **2021**. submitted manuscript.
29. Padmanabhan, S.; Katoa, S.; Nomura, K. Synthesis and Structure of Titanatranes Containing Tetradentate Trianionic Donor Ligands of the Type [(O-2,4-R<sub>2</sub>C<sub>6</sub>H<sub>2</sub>-6-CH<sub>2</sub>)<sub>2</sub>(OCH<sub>2</sub>CH<sub>2</sub>)]N<sub>3</sub>- and Their Use in Catalysis for Ethylene Polymerization. *Organometallics* **2007**, *26*, 1616–1626. [[CrossRef](#)]
30. Tshuva, E.Y.; Goldberg, I.; Kol, M.; Goldschmidt, Z. Living polymerization and block copolymerization of alpha-olefins by an amine bis(phenolate) titanium catalyst. *Chem. Commun.* **2001**, *20*, 2120–2121. [[CrossRef](#)]
31. Olmstead, M.M.; Power, P.P.; Viggiano, M. New class of sigma-bonded aliphatic aza-macrocylic complexes of transition metals: Synthesis and X-ray crystal structures of nitrogen-bridged [(TiN<sub>4</sub>C<sub>12</sub>H<sub>24</sub>)<sub>2</sub>] and the oxo-bridged species [(N<sub>4</sub>C<sub>12</sub>H<sub>25</sub>)TiOTi(N<sub>4</sub>C<sub>12</sub>H<sub>25</sub>)]. *J. Am. Chem. Soc.* **1983**, *105*, 2927–2928. [[CrossRef](#)]
32. Ugrinova, V.; Ellis, G.A.; Brown, S.N. Remarkable thermodynamic stability toward hydrolysis of tripodal titanium alkoxides. *Chem. Commun.* **2004**, 468–469. [[CrossRef](#)]
33. Nielson, A.J.; Shen, C.; Waters, J.M. Molecular engineering of coordination pockets in chloro-tris-phenoxo complexes of titanium(IV). *Polyhedron* **2006**, *25*, 2039–2054. [[CrossRef](#)]
34. Barroso, S.; Madeira, F.; Calhorda, M.J.; Ferreira, M.J.; Duarte, M.T.; Martins, A.M. Toward the understanding of radical reactions: Experimental and computational studies of titanium(III) diamine bis(phenolate) complexes. *Inorg. Chem.* **2013**, *52*, 9427–9439. [[CrossRef](#)] [[PubMed](#)]
35. Bernardinelli, G.; Seidel, T.M.; Kundig, E.P.; Prins, L.J.; Kolarovic, A.; Mba, M.; Pontini, M.; Licini, G. Stereoselective dimerization of racemic C<sub>3</sub>-symmetric Ti(IV) amine triphenolate complexes. *Dalton Trans.* **2007**, *16*, 1573–1576. [[CrossRef](#)] [[PubMed](#)]
36. Kremer, A.B.; Mehrkhodavandi, P. Dinuclear catalysts for the ring opening polymerization of lactide. *Coord. Chem. Rev.* **2019**, *380*, 35–57. [[CrossRef](#)]
37. Liang, L.C.; Chien, C.C.; Chen, M.T.; Lin, S.T. Zirconium and hafnium complexes containing N-alkyl-substituted amine biphenolate ligands: Unexpected ligand degradation and divergent complex constitutions governed by N-alkyls. *Inorg. Chem.* **2013**, *52*, 7709–7716. [[CrossRef](#)]
38. Toupance, T.; Dubberley, S.R.; Rees, N.H.; Tyrrell, B.R.; Mountford, P. Zirconium Complexes of Diamine–Bis(phenolate) Ligands: Synthesis, Structures, and Solution Dynamics. *Organometallics* **2002**, *21*, 1367–1382. [[CrossRef](#)]
39. Sun, Q.; Wang, Y.; Yuan, D.; Yao, Y.; Shen, Q. Zirconium complexes stabilized by amine-bridged bis(phenolato) ligands as precatalysts for intermolecular hydroamination reactions. *Dalton Trans.* **2015**, *44*, 20352–20360. [[CrossRef](#)]
40. Chmura, A.J.; Davidson, M.G.; Jones, M.D.; Lunn, M.D.; Mahon, M.F. Group 4 complexes of amine bis(phenolate)s and their application for the ring opening polymerisation of cyclic esters. *Dalton Trans.* **2006**, *7*, 887–889. [[CrossRef](#)]
41. Davidson, M.G.; Doherty, C.L.; Johnson, A.L.; Mahon, M.F. Isolation and characterisation of transition and main group metal complexes supported by hydrogen-bonded zwitterionic polyphenolic ligands. *Chem. Commun.* **2003**, *15*, 1832–1833. [[CrossRef](#)] [[PubMed](#)]
42. Wang, B.; Zhao, H.; Wang, L.; Sun, J.; Zhang, Y.; Cao, Z. Immortal ring-opening polymerization of lactides with super high monomer to catalyst ratios initiated by zirconium and titanium complexes containing multidentate amino-bis(phenolate) ligands. *New J. Chem.* **2017**, *41*, 5669–5677. [[CrossRef](#)]
43. Hu, M.; Wang, M.; Zhu, H.; Zhang, L.; Zhang, H.; Sun, L. Preparation and structures of enantiomeric dinuclear zirconium and hafnium complexes containing two homochiral N atoms, and their catalytic property for polymerization of rac-lactide. *Dalton Trans.* **2010**, *39*, 4440–4446. [[CrossRef](#)]
44. Whitelaw, E.L.; Jones, M.D.; Mahon, M.F.; Kociok-Kohn, G. Novel Ti(IV) and Zr(IV) complexes and their application in the ring-opening polymerisation of cyclic ester. *Dalton Trans.* **2009**, *41*, 9020–9025. [[CrossRef](#)] [[PubMed](#)]
45. Bisz, E.; Białek, M.; Zarychta, B. Synthesis, characterization and catalytic properties for olefin polymerization of two new dimeric zirconium(IV) complexes having diamine-bis(phenolate) and chloride ligands. *Appl. Catal. A* **2015**, *503*, 26–33. [[CrossRef](#)]
46. Forder, T.R.; Mahon, M.F.; Davidson, M.G.; Woodman, T.; Jones, M.D. Synthesis and characterisation of unsymmetrical Zr(IV) amine tris(phenolate) complexes and their application in ROP of rac-LA. *Dalton Trans.* **2014**, *43*, 12095–12099. [[CrossRef](#)] [[PubMed](#)]
47. Hornmairun, P.; Edward, L.M.; Vernon, C.G.; Robert, I.P.; White, A.J.P. Study of ligand substituent effects on the rate and stereoselectivity of lactide polymerization using aluminum salen-type initiators. *Proc. Natl. Acad. Sci. USA* **2006**, *103*, 15343–15348.
48. Pang, X.; Duan, R.; Li, X.; Chen, X. Bimetallic salen-aluminum complexes: Synthesis, characterization and their reactivity with rac-lactide and  $\epsilon$ -caprolactone. *Polym. Chem.* **2014**, *5*, 3894–3900. [[CrossRef](#)]
49. Chmura, A.J.; Cousins, D.M.; Davidson, M.G.; Jones, M.D.; Lunn, M.D.; Mahon, M.F. Robust chiral zirconium alkoxide initiators for the room-temperature stereoselective ring-opening polymerisation of rac-lactide. *Dalton Trans* **2008**, *11*, 1437–1443. [[CrossRef](#)]
50. McKeown, P.; Davidson, M.G.; Lowe, J.P.; Mahon, M.F.; Thomas, L.H.; Woodman, T.J.; Jones, M.D. Aminopiperidine based complexes for lactide polymerisation. *Dalton Trans.* **2016**, *45*, 5374–5387. [[CrossRef](#)]
51. Mandal, M.; Ramkumar, V.; Chakraborty, D. Salen complexes of zirconium and hafnium: Synthesis, structural characterization and polymerization studies. *Polym. Chem.* **2019**, *10*, 3444–3460. [[CrossRef](#)]

- 
52. Dubois, P.; Jacobs, C.; Jérôme, R.; Teyssié, P. Macromolecular Engineering of Polylactones and Polylactides. 4. Mechanism and Kinetics of Lactide Homopolymerization by Aluminum Isopropoxide. *Macromolecules* **1991**, *24*, 2266–2270. [[CrossRef](#)]
  53. Sheldrick, G.M. SHELXT—integrated space-group and crystal-structure determination. *Acta Crystallogr. A Found. Adv.* **2015**, *71*, 3–8. [[CrossRef](#)]
  54. Dolomanov, O.V.; Bourhis, L.J.; Gildea, R.J.; Howard, J.A.K.; Puschmann, H. OLEX2: A complete structure solution, refinement and analysis program. *J. Appl. Cryst.* **2009**, *42*, 339–341. [[CrossRef](#)]
  55. Sheldrick, G.M. Crystal structure refinement with SHELXL. *Acta Crystallogr. C Struct. Chem.* **2015**, *71*, 3–8. [[CrossRef](#)] [[PubMed](#)]
  56. Macrae, C.F.; Edgington, P.R.; McCabe, P.; Pidcock, E.; Shields, G.P.; Taylor, R.; Towler, M.; Streek, J.v.d. Mercury: Visualization and analysis of crystal structures. *J. Appl. Cryst.* **2006**, *39*, 453–457. [[CrossRef](#)]